Proceedings of the 17th World Congress
The International Federation of Automatic Control
Seoul, Korea, July 6-11, 2008

Design of Seeking Control Based on Two-Degree-of-Freedom Controller Using Frequency Shaped Final-State Control

Hyun Jae Kang*, Choong Woo Lee*, Chung Choo Chung† and Ho-Seong Lee*****

**Department of Electrical and Computer Engineering, Hanyang University, Seoul, 133-791, Korea, (e-mail: hyunjae.kang@ gmail.com, chungwoo73@yahoo.co.kr).*
*** Division of Electrical and Biomedical Engineering, Hanyang University, Seoul, 133-791, Korea, (Tel: +82-2-2220-1724; e-mail: cchung@hanyang.ac.kr)*
**** Storage System Division, Semiconductor Business, Samsung Electronics, Suwon,443-742, Korea, (e-mail: hoseong.lee@samsung.com)*

Abstract: In this paper, we introduce a new seeking control method based on the frequency shaped final-state control (FFSC). The seeking control method is a two-degree-of-freedom control, which is the plant-based feedforward control. The feedforward control input is designed through zero-order-hold using FFSC which imposes the constraints on control input magnitude and its frequency components to minimize residual vibrations. The reference generation is made through a feedforward path controller which is in the form of the zero-phase error tracking controller (ZPETC) of the nominal plant. The reference prefilter is designed to compensate the delay in the control system via the ZPETC. Mode switching control (MSC) is employed to enhance tracking performance after settling. An add-on type disturbance observer that is in the form of finite impulse response is used with the feedback controller. From the simulation results, the proposed method shows the improvement to the settling and disturbance rejection.

1. INTRODUCTION

The issue with respect to fast seeking and settling performance is how to reduce residual vibrations caused by plant's resonance modes. Several methods have been proposed to avoid the residual vibrations: The SMART control (Mizoshita *et al.,* 1996) is proposed for designing a trajectory that minimizes a jerk during seeking. An augmented band reject filter (BRF) with the final-state control (FSC) is also used to reduce the energy in control input at a certain frequency band (Okuyama *et al.,* 2005). Using LMI constraints to limit the energy of the control intput at a certain frequency band and the amplitude of the control command is proposed to avoid resonance mode excitation (Hirata *et al.,* 2002).

To acquire the inverse dynamics of a plant having unstable zeros, the zero phase error tracking controller (ZPETC) has been proposed to compensate the non-minimum phase effect of unstable zeros (Tomizuka, 1987). In addition, to improve tracking capability, ZPETC with multi-rate sampling technique is proposed (Kobayashi *et al.,* 1998). The ZPETC can cancel phase error. However, gain error caused by the unstable zeros remains. To compensate both gain and phase errors, the perfect tracking control (PTC) based on multi-rate sampling technique has been proposed (Fujimoto *et al.,* 2001).

The FSC is known to be effective in generating a discrete-time trajectory with zero-order hold (ZOH). To minimize a certain frequency component of the FSC input, the frequency shaped final-state control (FFSC) is proposed (Hirata *et al.,* 2002). In the FFSC, the two-degree-of-freedom (TDOF) control scheme is effective because actual systems have various disturbances and plant uncertainties. However, the conventional TDOF control has a limitation in improving the performance because of inaccurate modelling of high frequency resonance modes (Hirata, 2005).

In this paper, we introduce a new seeking control method based on the FFSC. The seeking control method is a TDOF control, which is the plant-based feedforward control (Ellis, 2004). The feedforward control input is designed through ZOH using the FFSC which imposes the constraints on control input magnitude and its frequency components to minimize residual vibrations. The reference generation is made through a feedforward path controller which is in the form of the ZPETC of the nominal plant. The reference prefilter similar to the closed-loop inverse (CLI) architecture (Rigney *et al.,* 2006) is designed to compensate the delay in the control system via the ZPETC.

Even TDOF control in the FFSC may increase position error signal (PES) at the arrival of the desired position by the neglected vibration mode. To overcome this problem, two methods are proposed adding a static gain and verified with experimental data (Hirata, 2005). In this paper, an add-on type disturbance observer (DOB) in the form of finite impulse response (FIR) is used with a feedback controller (Suh *et al.,* 2002). This is a kind of mode switching control (MSC) different from the conventional MSC (Yamaguchi *et al.,* 1996)(Okuyama *et al.,* 2005). The conventional MSC uses two controllers and switching between the controllers is made when the objective of the control changes. Instead, the proposed MSC uses the add-on type DOB only during

†*Corresponding author*. e-mail: cchung@hanyang.ac.kr

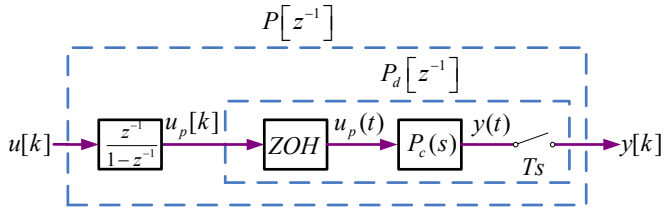

Fig. 1 Augmented system

tracking mode after settling. In other words, the DOB is switched off during seeking and turned on in the beginning of tracking. The proposed MSC does not need the initial value compensation (IVC) necessary for the conventional MSC (Yamaguchi *et al.,* 1996).

In a summary, first, in order to minimize the excitation of the plant's resonance modes, a convex optimization technique is used for minimizing the energy of the control input in the frequency band where the resonance modes exist (Wu *et al.,* 2005)(Hirata *et al,*. 2002). Second, a new design of TDOF controller via the plant-based feedforward control is implemented. Third, in order to reject disturbances, an add-on type DOB is used. From simulation results we validated the performance of the proposed method with the improved fast settling time and tracking performance while rejecting disturbances.

2. TRAJECTORY GENERATION VIA CONVEX OPTIMIZATION

In this section, we describe how to design a trajectory that minimizes the excitation of the plant resonance modes. This is a summary of related works (Hirata *et al.,* 2002) (Wu *et al.,* 2005). Energy minimization is performed by imposing the constraints on control input magnitude and its frequency components. Compared to BRF approach (Okuyama *et al.,* 2005), the advantage of this method is effectively to reject the energy of control input at a certain wide bandwidth. Its performance is robust against model uncertainty.

2.1 Final-State Control

An integrator to avoid jerk in the control input is added as illustrated in Fig. 1. $P_c(s)$ is the plant transfer function in the continuous-time domain. And its state-space representation is given by

$$\dot{x}_c(t) = A_c x_c(t) + B_c u_p(t)$$
$$y(t) = C_c x_c(t).$$

$P_d[z^{-1}]$ is a discrete-time model of $P_c(s)$ using zero-order hold (ZOH) equivalence and its state-space equation is expressed by

$$x_d[k+1] = A_d x_d[k] + B_d u_p[k]$$
$$y[k] = C_d x_d[k].$$

Then the state-space equation of the augmented system $P[z^{-1}]$ including the integrator becomes

$$x_d[k+1] = Ax[k] + Bu[k]$$
$$y[k] = Cx[k] \tag{1}$$

where

$$A = \begin{bmatrix} A_d & B_d \\ 0 & 1 \end{bmatrix},\ B = \begin{bmatrix} 0 \\ 1 \end{bmatrix},\ C = \begin{bmatrix} C_d & 0 \end{bmatrix},\ x[k] = \begin{bmatrix} x_d[k] \\ u_p[k] \end{bmatrix}.$$

Assume that *(A, B)* is controllable. Then it is possible to obtain a set of control inputs which drives the initial state $x[0] = x_0$ to the final state $x[N] = x_{des}$. Such inputs are not unique in general. The minimum energy optimal control problem is to choose the inputs $u[0]$, $u[1]$, … , $u[N-1]$ so as to minimize the total energy, J of the input signals, i.e.,

$$J = \min \sum_{k=0}^{N-1} u[k]^2 \tag{2}$$

To formulate it as a convex optimization problem, define U as the stack of the input signal $u[k]$ such as

$$U = \begin{bmatrix} u[0] & u[1] & \cdots & u[N-1] \end{bmatrix}^T$$

$$\Sigma = \begin{bmatrix} A^{N-1}B & A^{N-2}B & \cdots & B \end{bmatrix}.$$

Since the control input $u[k]$ must drive the state-variable $x[k]$ from x_0 to x_{des}, from (1) we see that

$$\Sigma U = x_{des} - A^N x_0 . \tag{3}$$

This is a linear equality constraint on U. The control input which minimizes the total energy, J subject to (3) becomes

$$U = \Sigma^T \left(\Sigma\Sigma^T\right)^{-1} \left(x[N] - A^N x[0]\right).$$

2.2 Magnitude constraints

Define $z[k]$ the combination of state $x[k]$ and control input signal $u[k]$. Then we have

$$z[k] = C_z x[k] + D_z u[k] \tag{4}$$

where

$$C_z = \begin{bmatrix} 0 & 0 & 1 \end{bmatrix},\ D_z = 0 .$$

From (1) and (4), Z can be expressed as an affine function of U such as

$$Z = \Phi_z x_0 + \Omega_z U$$

where

$$\Phi_z = \begin{bmatrix} C_z \\ C_z A \\ \vdots \\ C_z A^{N-1} \end{bmatrix},\ \Omega_z = \begin{bmatrix} D_z & 0 & \cdots & 0 \\ C_z B & D_z & \ddots & \vdots \\ \vdots & \ddots & \ddots & 0 \\ C_z A^{N-2} B & \cdots & C_z B & D_z \end{bmatrix},$$

$$Z = \begin{bmatrix} z[0] & z[1] & \cdots & z[N-1] \end{bmatrix}^T .$$

Due to physical constraints on the control input, we obtain the linear inequality constraints of U such as

$$Z_{\min} \le \Phi_z x_0 + \Omega_z U \le Z_{\max} . \quad (5)$$

2.3 Frequency constraints

The Fourier transformation $\hat{Z}(j\Omega)$ of $z(t)$ becomes

$$\hat{Z}(j\Omega) = \int_0^{NT_s} z(t) e^{-j\Omega t} dt . \quad (6)$$

Here, $z(t)$ can be also rewritten as

$$z(t) = \sum_{k=0}^{N-1} z[k] h_0(t - kT_s) \quad (7)$$

and $h_0(t)$ is the impulse response of the ZOH. In (6) and (7), the Fourier transform can be shown as

$$\begin{aligned} \hat{Z}(j\Omega) &= \sum_{k=0}^{N-1} z[k] H_0(j\Omega) e^{-j\Omega kT} \\ &= W(j\Omega) Z. \end{aligned} \quad (8)$$

Here, $W(j\Omega)$ is defined as

$$W(j\Omega) = H_o(j\Omega) \begin{bmatrix} 1 & e^{-j\Omega T_s} & e^{-j\Omega 2T_s} & \cdots & e^{-j\Omega(N-1)T_s} \end{bmatrix} . \quad (9)$$

The frequency response of ZOH is

$$H_0(j\Omega) = \frac{2\sin(\Omega T_s / 2)}{\Omega} e^{-j\Omega T_s / 2} .$$

An energy limitation to $\hat{Z}(j\Omega)$ at a certain frequency Ω_i can be formulated as

$$\left| \hat{Z}(j\Omega_i) \right|^2 \le q_i^2 . \quad (10)$$

Here, if (8) and (10) are arranged by dividing $W(j\Omega)$ into real numbers and imaginary numbers, we get

$$Z^T \left(W_R^T(j\Omega_i) W_R(j\Omega_i) + W_I(j\Omega_i)^T W_I(j\Omega_i) \right) Z \le q_i^2 .$$

Z is an affine function of U so that the above equation becomes the quadratic constrain of U. The convex optimization problem with variable $u[k]$ for $k = 0, \ldots, N - 1$ and $U = [u[0], u[1], \ldots, u[N - 1]]^T$ can be expressed by

$$\begin{aligned} &\min \|U\|_2^2 \\ &\textit{subject to } \Sigma U = x_{des} - A^N x_0 \\ &\qquad u_{\min} \le U_p \le u_{\max} \\ &\qquad U_p^T (W_R^T(j\Omega_i) W_R(j\Omega_i) \\ &\qquad + W_I(j\Omega_i)^T W_I(j\Omega_i)) U_p \le q_i^2, \ (i = 1, \ldots, M) \\ &\textit{where } U_p = \Phi_z x_0 + \Omega_z U \end{aligned}$$

Fig. 2 Conventional ZPETC structure

This problem is a quadratic constrained quadratic program (QCQP) (Boyd *et al.,* 2004).

3. A NEW FEEDFORWARD STRUCTURE

We described how the feedforward control input is designed through ZOH using the FFSC. In this section, we present a plant-based feedforward control which consists of a feedforward path controller and a reference prefilter. The reference generation, $r[k]$ is made through the feedforward path controller which is the ZPETC of the nominal plant. The reference prefilter placed in front of the reference input, $r[k]$ is used to compensate the delay in the control system via the ZPETC.

3.1 Design of the feedforward path controller, $P_Z[z^{-1}]$

Fig. 2 describes the structure of conventional ZPETC. Suppose that the closed-loop transfer function, which includes the controlled plant and feedback controller, is expressed as

$$G_{cl}[z^{-1}] = \frac{z^{-d} B(z^{-1})}{A(z^{-1})} .$$

where z^{-d} represents a d-step delay normally caused by the delay in the plant. $B(z^{-1})$ is factorized into two parts: $B^+(z^{-1})$ includes zeros of the closed-loop system inside of the unit circle. $B^-(z^{-1})$ does those outside of the unit circle bearing uncancellable zeros. Then the conventional ZPETC has the following transfer function (Tomizuka, 1987)

$$G_Z[z^{-1}] = \frac{z^{d+s} A(z^{-1}) B^-(z)}{B^+(z^{-1}) \{B^-(1)\}^2} .$$

where s is the number of the uncancellable zeros. The subscript z indicates ZPETC. The conventional ZPETC cancels the poles and cancellable zeros of the closed-loop system, and compensates for the phase shift induced by uncancellable zeros. The discrete time model, $P_d[z^{-1}]$ of a plant with a plant delay may possess unstable zeros. In this paper, the feedforward path controller for the reference generation in Fig. 3(a) is obtained using the ZPETC, $P_Z[z^{-1}]$.

3.2 Design of the reference prefilter controller, $G_{ff}[z^{-1}]$

From redrawing the block diagram in Fig. 3(a) to get the block diagram in Fig. 3(c), we see that Fig. 3(c) is equivalent to Fig. 2. Then we can induce that $G_{ff}[z^{-1}]$ can be obtained from (11).

$$G_{ff}[z^{-1}] = G_Z[z^{-1}] - P_Z[z^{-1}] C_Z[z^{-1}] \quad (11)$$

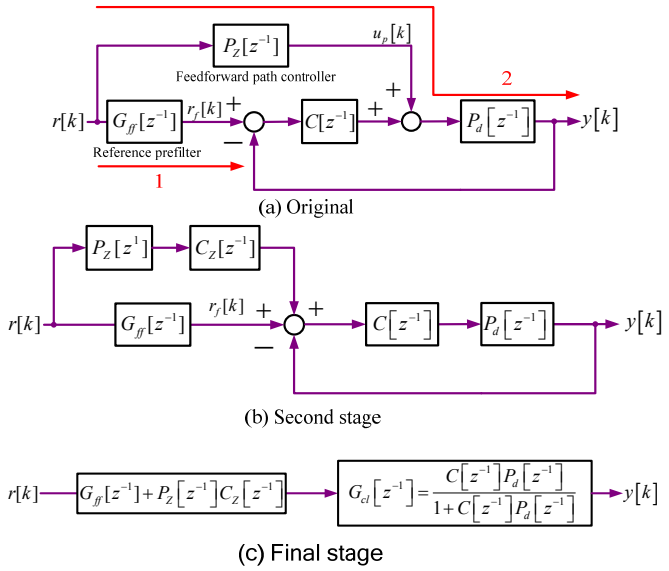

Fig. 3 The Proposed ZPETC structure for plant-based feedforward control

where $P_Z[z^{-1}]$ and $C_Z[z^{-1}]$ are the ZPETC of the plant $P_d[z^{-1}]$ with a plant delay and that of the feedback controller $C[z^{-1}]$, respectively.

***Remark* 1**. $G_{ff}[z^{-1}]$ compensates the command delay in the control system from the reference input $r[k]$ to the output $y[k]$.

***Claim* 1**. $G_{ff}[z^{-1}]$ can be independently designed regardless of the feedback controller $C[z^{-1}]$.

Using simple algebra on ZPETC we can easily prove claim 1. To obtain the same phase on $r_f[k]$ and $y[k]$, it is clear that

$$G_{ff}\left[z^{-1}\right]=P_d\left[z^{-1}\right]P_Z\left[z^{-1}\right]. \tag{12}$$

Equation (12) means that the phase of the path 1 is the same as that of the path 2 in Fig. 3(a). In other words, the phase of $r_f[k]$ is the same as that of $y[k]$. Subsequently, the phase of input $r[k]$ is the same as that of output $y[k]$. We will provide a sketch of the proof of the claim as follows.

The transfer function of block diagram in Fig. 3(c) is

$$y[k]=\left(G_{ff}\left[z^{-1}\right]+P_Z\left[z^{-1}\right]C_Z\left[z^{-1}\right]\right)G_{cl}\left[z^{-1}\right]r[k] \tag{13}$$

Substituting (12) into (13), we have the following description.

$$y[k]=\left(P_d\left[z^{-1}\right]P_Z\left[z^{-1}\right]+P_Z\left[z^{-1}\right]C_Z\left[z^{-1}\right]\right)G_{cl}\left[z^{-1}\right]r[k] \tag{14}$$

Assuming the control signal is within the bandwidth of the feedback controller $C[z^{-1}]$, then we see that

$$P_Z\left[z^{-1}\right]P_d\left[z^{-1}\right]=P_Z\left[z^{-1}\right]P_d\left[z^{-1}\right]C_Z\left[z^{-1}\right]C\left[z^{-1}\right] \tag{15}$$

Substituting (15) into (14), we obtain (16).

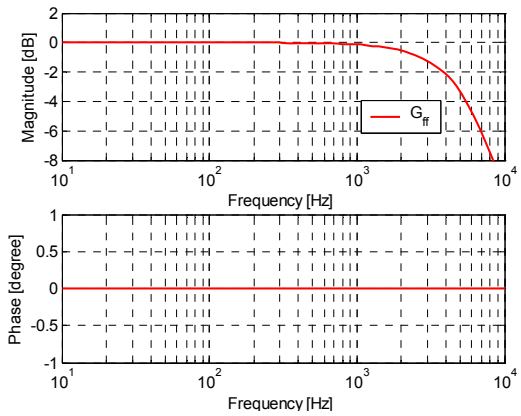

Fig. 4 Bode plot of reference prefilter, $G_{ff}[z^{-1}]$

$$y[k]=\left(P_Z\left[z^{-1}\right]P_d\left[z^{-1}\right]C_Z\left[z^{-1}\right]C\left[z^{-1}\right]\right)r[k] \tag{16}$$

Accordingly, the reference prefilter, $G_{ff}[z^{-1}]$ compensates the command delay from the input $r[k]$ to the output $y[k]$. This is similar to ZPETC with the closed-loop inverse (CLI) architecture (Rigney *et al.,* 2006). The reference prefilter, $G_{ff}[z^{-1}]$ is independent of the feedback controller $C[z^{-1}]$. The bode plot of $G_{ff}[z^{-1}]$ is illustrated in Fig. 4.

Remark 2. $G_{ff}[z^{-1}]$ is in the form of

$$G_{ff}\left[z^{-1}\right]=\frac{z^{s}B^{-}\left[z^{-1}\right]B^{-}\left[z\right]}{B^{-}\left[1\right]^{2}}$$

$G_{ff}[z^{-1}]$ is a non-causal system and has a finite impulse response. The magnitude is 0dB which does not affect the system gain.

4. MODE SWITCHING CONTROL

In this section, we introduce MSC. Fig. 5 illustrates the seeking/settling and tracking control system. The feedforward path controller and reference prefilter are designed to improve seeking and settling performance. The feedback controller and add-on type DOB (Suh *et al.,* 2002) are designed to improve the tracking performance rejecting disturbances. The proposed MSC is different from the conventional MSC. In the conventional MSC, IVC method to improve transient characteristics after mode switching is needed. Instead, the proposed MSC uses the add-on type DOB only during tracking mode. In other words, the feedforward path controller and reference prefilter for the seeking and settling are always turned on. The DOB is switched off during the seeking and settling, and turned on in the beginning of tracking. The proposed MSC does not need the IVC like the conventional MSC (Yamaguchi *et al.,* 1996).

5. SIMULATION RESULTS

In this section, we will present simulation results with a numerical example. The plant is a positioner used in servo track writer (STW) system. The positioner is actuated by a voice-coil-motor.

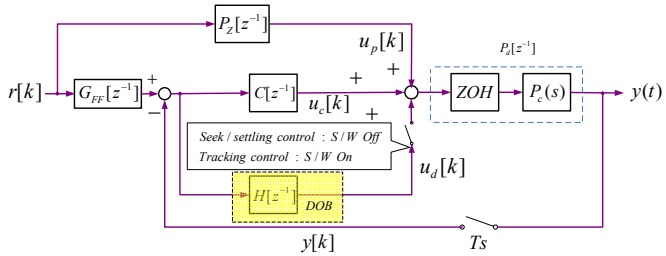

Fig. 5 Seeking/settling and tracking control structure

5.1 Simulation conditions

The sampling frequency is 20 kHz and the initial and final states of the plant are as follows:

$$\left[x_{pos}[0] \quad x_{vel}[0] \quad x_{acc}[0]\right]^T = [0 \quad 0 \quad 0]^T$$

$$\left[x_{pos}[N] \quad x_{vel}[N] \quad x_{acc}[N]\right]^T = [835 \quad 0 \quad 0]^T$$

Here, the state variable x_{pos} is the position and its unit is [count]. $x_{pos}[N]$ is set as 835[count]. x_{vel} is the velocity and x_{acc} is the acceleration. The plant's resonance exists at 6.515 kHz, therefore in order to reject its vibration, frequency constraints were given by adjusting the value of q_i in (10) from 5.72 kHz to 7.02 kHz. Ω_i was chosen as (18).

$$\Omega_i = \Omega_l + \frac{\Omega_u - \Omega_l}{M-1} i, \quad i = 1, \ldots, M \tag{18}$$

Here, $\Omega_l = 5.72 \times 2\pi$ and $\Omega_u = 7.02 \times 2\pi$, and the YALMIP Toolbox of MATLAB/Simulink™ was used to compute the control input $u_p[k]$ (Löfberg *et al.,* 2004).

5.2 Trajectory generation via convex optimization

Fig. 6 show that the reference $r[k]$ is generated based on the feedforward path control input $u_p[k]$ with the plant model $P_d[z^{-1}]$. Fig. 7(a) compares the control inputs $u_p[k]$ when frequency constraints are given and not given. The desired settling time is 1*ms* (N=20). The frequency spectrum of $u_p[k]$ is shown in Fig. 7(b). From this figure, we see that the frequency constraints on control inputs push down the energy of the control input around the resonance mode. Instead, the energy at low frequency is slightly increased. The energy is spilled over to other frequency ranges due to the constraints. From Fig. 7(b), notice that the energy of the control command around the resonance mode is minimized.

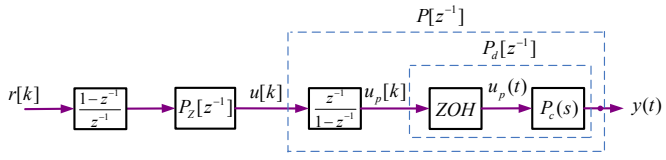

Fig. 6 Trajectory generation structure

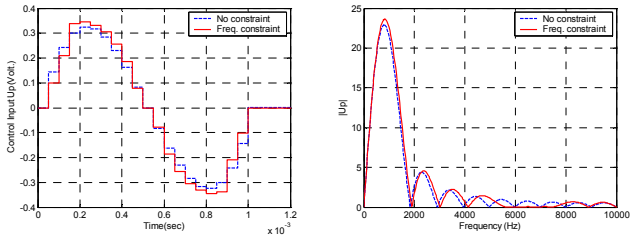

(a) Control input, $u_p[k]$ (b) Frequency spectrum

Fig. 7 Control input and its frequency spectrum

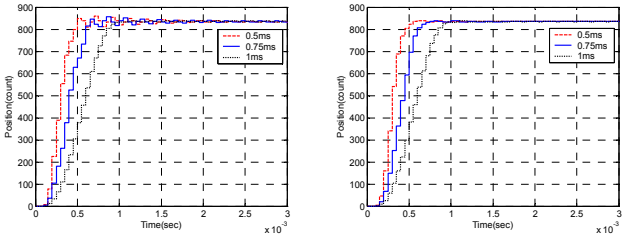

(a) Minimum energy (b) Proposed method

Fig. 8 The seeking motion: (a) min. energy (b) the proposed method using minimum energy with frequency constraints

We simulated for three different cases to see how the resonance mode is excited. The desired settling times were set as 1, 0.75, 0.5*ms* (N=20, 15, 10). Fig. 8(a) illustrates the seeking performance only with energy optimization. Resonance mode was excited for the all three cases. We see that the earlier the desired settling time is, the more resonance mode is excited. Fig. 8(b) shows the energy optimization with frequency constraints. In this case, although the desired settling time is reduced, the resonance mode is hardly excited compared to Fig. 8(a). The effect of energy optimization with frequency constraints becomes distinctive as the settling time is reduced.

5.3 Reference prefilter

We used the proposed ZPETC structure in section 3. We consider the effect of plant delay 20 *u*s caused by the plant in Fig. 5 and the desired settling time is set as 0.75*ms*. In Fig. 9 PESs with $G_{ff}[z^{-1}]$ designed by ZPETC and $G_{ff}[z^{-1}]$=1 are plotted. Settling time without $G_{ff}[z^{-1}]$ is slower than the desired one caused by the plant time delay. When applying the proposed $G_{ff}[z^{-1}]$, we get the settling time, 1 *ms*.

5.4 Seeking/settling and tracking control

The whole system was constructed as shown in Fig. 5. To evaluate the performance of the DOB, we injected the input disturbance of 120 Hz into the system. Fig. 10 shows PES for 835 [count] seeking. The dashed line shows the control input with energy minimization, the solid line shows the control input with energy minimized and frequency constraints, and the dotted line shows input energy minimization with frequency constraints and the DOB. The transient response is improved with frequency constrains.

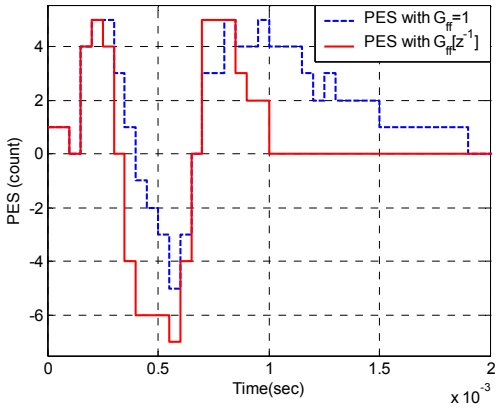

Fig. 9 PES's of with $G_{ff}[z^{-1}]$=1 and with $G_{ff}[z^{-1}]$

This is because the control input energy at the frequency where the plant's resonance mode exists was minimized. From Fig. 10(b), the dotted line with the use of the DOB shows less vibration than the dashed line and solid line without the DOB. This is because the low frequency disturbance was effectively removed by the DOB. Fig. 11(a) shows the FFT of PES's in the range of 5000Hz to 7500Hz. The frequency constraints around the frequency band of 6515Hz where the resonance mode exists has decreased. Fig. 11(b) shows the FFT of PES's in the range of 0Hz to 250Hz. The energy around the frequency band of 120Hz where the low frequency disturbance exists has also been decreased with the DOB.

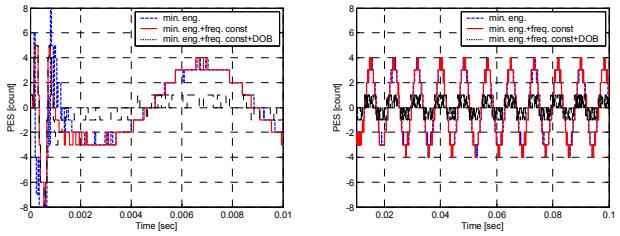

Fig. 10 PES: (a) 0sec~0.01sec, (b) 0.01sec~0.1sec

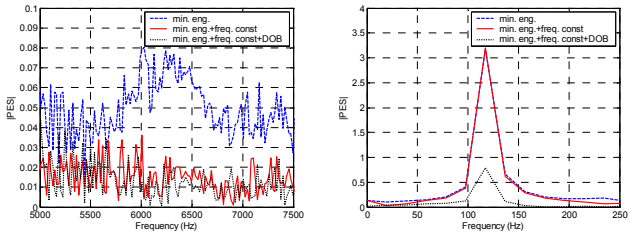

Fig. 11 FFT of PES: (a) 5000Hz~7500Hz, (b) 0Hz~250Hz

6. CONCLUSIONS

In this paper, we have proposed a new seeking control method based on the FFSC. A convex optimization technique was used for minimizing the energy of the control input in the frequency band where the resonance modes exist. The seeking control method is the TDOF control which uses the plant-based feedforward control. An add-on type DOB was used for tracking performance enhancement after settling. From simulation results we validated the performance of the proposed method. The proposed method can be effectively applied to STWs which use a fixed seeking length.

REFERENCES

Boyd, S. and L. Vandenberghe (2004). *Convex Optimization,* Cambridge University Press.

Ellis, G. (2004). *Control system design guide*, Elsevier Academic Press.

Fujimoto, H., Y. Hory and A. Kawamura (2001). Perfect tracking control based on multirate feedforward control with generalized sampling peroids. *IEEE Trans. on Industrial Electronics,* **VOL. 48, NO. 3** , pp. 636-644 .

Hirata, M., T. Hasegawa and K. Nonami (2002). Seek Control of Hard Disk Drives Based on Final-State Control Taking Account of the Frequency Components and the Magnitude of Control Input. *In Proc. of Advanced Motion Control,* pp. 40-45.

Hirata, M. (2005). Track seeking control of hard disk drives based on new two-degree-of-freedom control scheme with vibration minimized trajectory, *16th IFAC World Congress*.

Kobayashi, M., T. Yamaguchi, I. Oshimi, Y. Soyama, H. Hirai (1998). Multi-rate zero phase error feedforward control for magnetic disk drives. *In: Conference on information, intelligence and precision equipment (IIP' 98)*, **No. 98 -26**, pp. 21-22

Löfberg, J. (2004). YALMIP:A toolbox for modeling and optimization in MATLAB. *In Proceedings of the CACSD Conference, Taipei, Taiwan,* pp. 284-289.

Mizoshita, Y., S. Hasegawa and K. Takaishi (1996). Vibration Minimized Access Control for Disk Drives. *IEEE Trans. on Mag.,* **VOL. 32, NO. 3,** pp. 1793-1798.

Okuyama, A., M. Kobayashi, T. Horiguchi and K. Shishida (2005). A design based on final-state control for residual vibrationless seeking in hard disk drives. *Microsystem Technologies,* **VOL. 11, NO. 8-10,** pp. 688-695.

Rigney, B., L. Pao, and D. A. Lawrence (2006), Settle time performance comparisons of stable approximate model inversion techniques, *In Proceedings of the American Control Conference, Minnesota, USA,* pp. 600-605.

Suh,S.-M., C.C. Chung and S.-H. Lee (2002). Discrete-time track following controller design using a state-space disturbance observer. *Microsystem Technologies,* **VOL. 9, NO. 5,** pp. 352-361.

Tomizuka, M. (1987). Zero Phase Error Tracking Algorithm for Digital Control. *ASME, J. Dynam. Syst. Meas. Control,* **VOL. 109, NO. 1,** pp. 65-68.

Wu, S.-C. (2005). Optimal Design of Feedforward Control Input for Settling Control in Hard Disk Drives. *Unpublished*.

Yamaguchi, T., Y. Soyam, H. Hosokawa, K. Tsuneta and H. Hirai (1996). Improvement of Settling Response of Disk Drive Head Positioning Servo using Mode Switching Control with Initial Value Compensation. *IEEE Trans. on Mag.,* **VOL. 32, NO. 3,** pp. 1767-1772.